Complex Signal Kurtosis and Independent Component Analysis for Wideband Radio Frequency Interference Detection

Adam Schoenwald (ASRC Federal Space and Defense)

Dr. Priscilla Mohammed, (Morgan State University)
Dr. Damon Bradley (NASA, GSFC)
Dr. Jeffrey Piepmeier (NASA, GSFC)
Dr. Englin Wong (NASA, GSFC)
Dr. Armen Gholian (NASA, GSFC)

To be presented by Adam Schoenwald at Coexisting with Radio Frequency Interference, Socorro NM, October 17-20, 2016

Acronym List

Acronym	Definition
ABS()	Absolute Value
AS&D	ASRC Federal Space and Defense
AUC	Area Under Curve
CERBM	Complex Entropy Rate Bound Minimization
CONUS	Continental United States
CQAMSYM	Complex Quadrature Amplitude Modulation
CSK	Complex Signal Kurtosis
CW	Continuous Wave
dB	Decibel
DDC	Digital Down Converter
DSP	Digital Signal Processing
DVB-S2	Digital Video Broadcasting - Satellite - Second Generation
ERBM	Entropy Rate Bound Minimization
ESTO	Earth Science Technology Office
FB	Full Band
FPGA	Field Programmable Gate Array
Gbps	Billions of Bits per Second
GMI	GPM Microwave Imager
GPM	Global Precipitation Measurement

Acronym	Definition
GSFC	Goddard Space Flight Center
H	Horrizontal
ICA	Independent Component Analysis
INR	Interference to Noise Ratio
NASA	National Aeronautics and Space Administration
NCCFASTICA	Non Circular Complex Fast ICA
PI	Principal Investigator
QPSK	Quadrature Phase Shift Keying)
RADAR	RAdio Detection And Ranging
RF	Radio Frequency
RFI	Radio Frequency Interference
ROACH	Reconfigurable Open Architecture Computing Hardware
ROC	Receiver Operating Characteristic
RRCOS	Root Raise Cosine
RSK	Real Signal Kurtosis
SB	Sub Band
SERDES	Serializer / Deserializer
SMAP	Soil Moisture Active Passive
V	Vertical

Motivation

- Unmitigated RFI (Radio Frequency Interference) can cause errors in science measurements
  - L- and C-Band: soil moisture measurements over land
  - L-, C- and X-band: ocean salinity, sea surface temperature, wind speed direction
  - K band: water vapor, liquid water
- Approach
  - RF front end development for 18 GHz (K band)
    - These allocations are known to be corrupted by direct broadcast services
  - Digital back end to allow sophisticated RFI detection and mitigation techniques

L, X band RFI

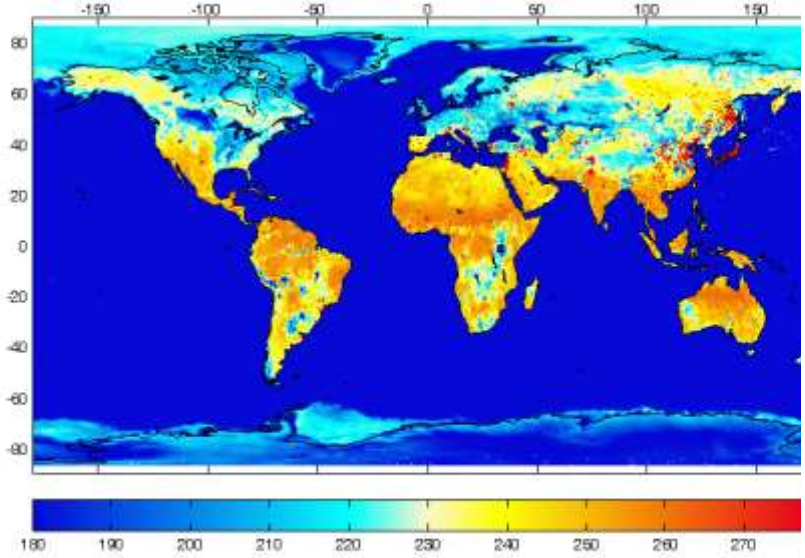

SMAP TA H-pol
1400 MHz

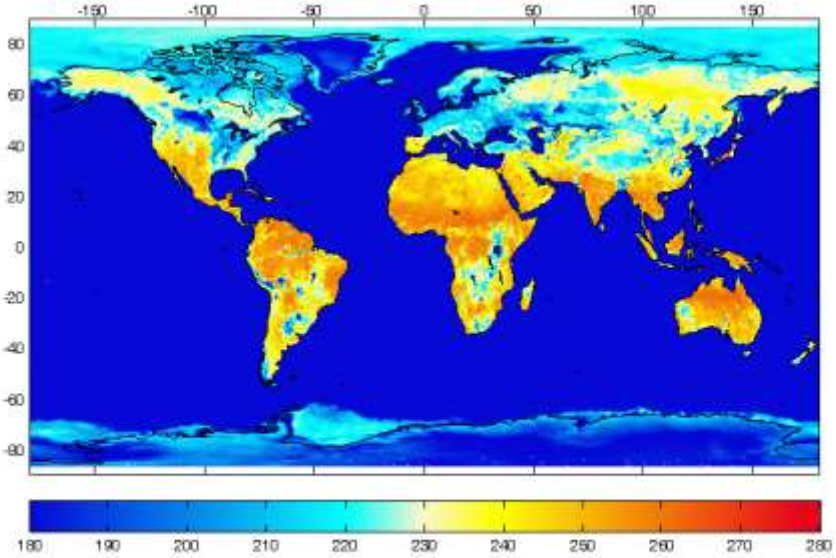

SMAP TA H-pol filtered

10 GHz GMI
Tb V-pol
(Vertical)

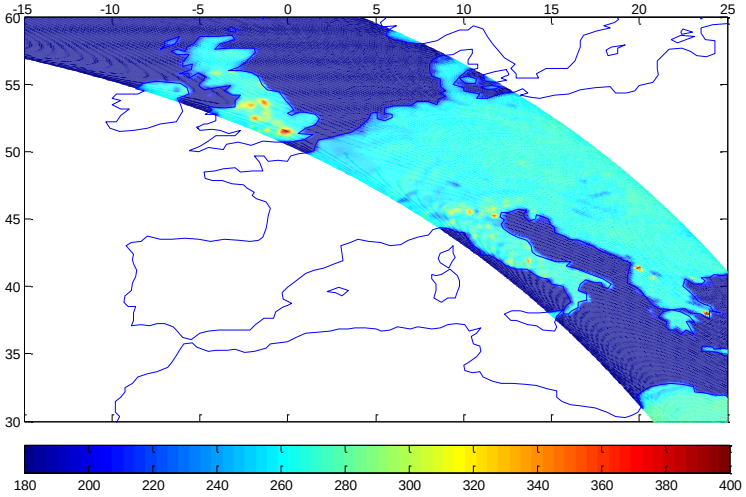

SMAP (Soil Moisture Active Passive) algorithms developed previously under ESTO (Earth Science Technology Office)

RFI from Geosynchronous Satellites Reflecting from the Surface

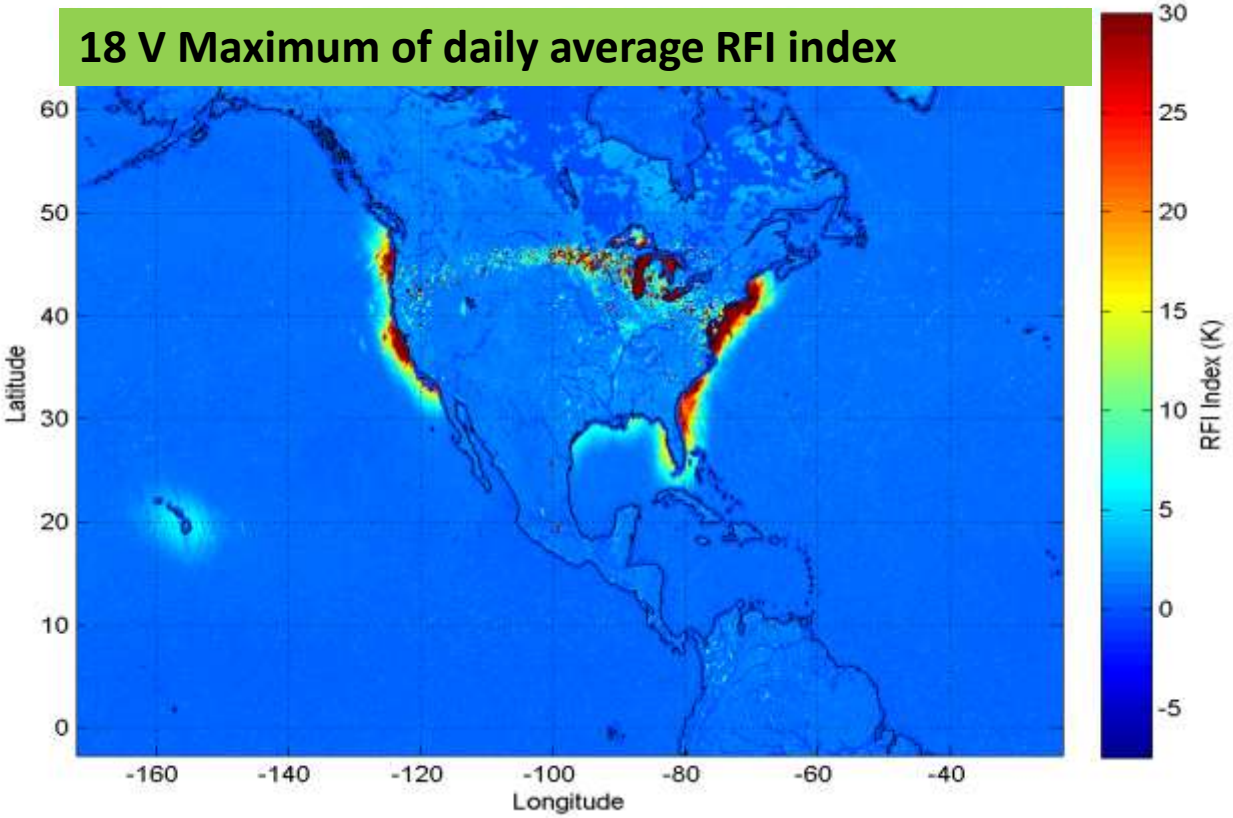

GMI data

Picture from David W. Draper, [1]

The 18 GHz Channel sees significant RFI from surface reflections around CONUS (Continental United States) and Hawaii

Real Signal Kurtosis (RSK)

Based on Thermal Noise Amplitude Probability Distribution

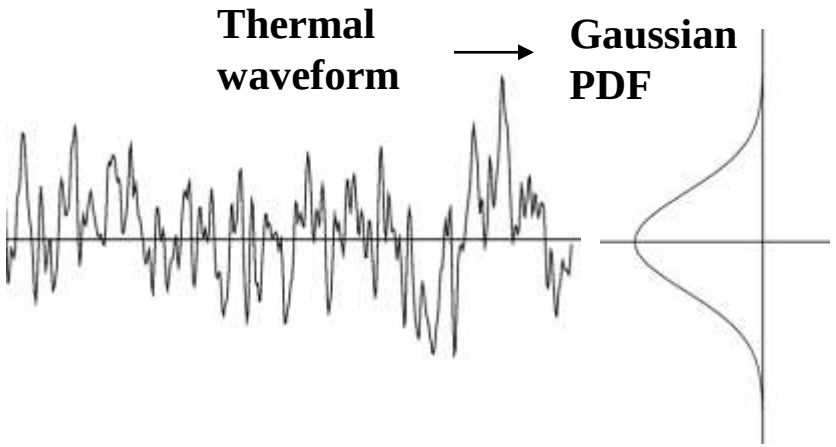

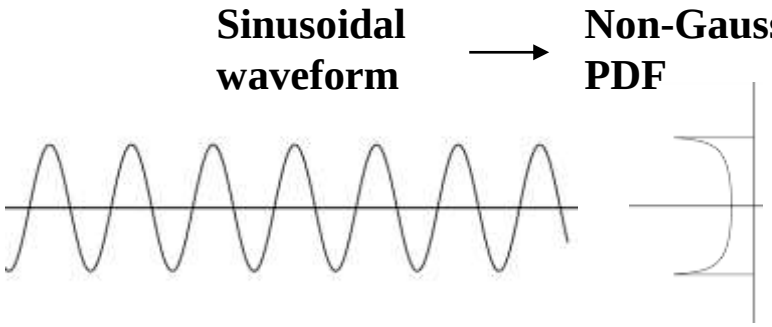

Sketches of noise and sinusoidal waveforms/PDFs

K = 3 for Gaussian signal

Figure from [2]

$$K \equiv \frac{E[(x-\bar{x})^4]}{E[(x-\bar{x})^2]^2} = \frac{m_4 - 4m_1m_3 + 6m_1^2m_2 - 3m_1^4}{m_2^2 - 2m_2m_1^2 + m_1^4} \qquad \sigma_K = \sqrt{\frac{24}{B\tau}}$$

RSK [2] is used on SMAP [3] to help flag measurements that are contaminated with RFI

Real Signal Kurtosis (RSK)

Given a complex baseband signal $z(n) = I(n) + jQ(n)$, the fourth standardized moment is computed independently for both the real and imaginary vectors, I and Q, as was used in SMAP[3].

$$\mathrm{RSK_I} = \frac{\mathbb{E}[(\mathrm{I}-\mathbb{E}[\mathrm{I}])^4]}{(\mathbb{E}[(\mathrm{I}-\mathbb{E}[\mathrm{I}])])^2} - 3 \quad , \quad \mathrm{RSK_Q} = \frac{\mathbb{E}[(\mathrm{Q}-\mathbb{E}[\mathrm{Q}])^4]}{(\mathbb{E}[(\mathrm{Q}-\mathbb{E}[\mathrm{Q}])])^2} - 3$$

The test statistic, RSK [2,3] (Real Signal Kurtosis), is then defined as

$$\mathrm{RSK} = \frac{|\mathrm{RSK_I}| + |RSK_Q|}{2}$$

Complex Signal Kurtosis

Complex signal kurtosis (CSK) [4] is used to improve ability of the digital radiometer to detect RFI. It makes use of additional information in complex signals.

Given a complex baseband signal $z(n) = I(n) + jQ(n)$, *moments* $\alpha_{\ell,m}$ of $z(n)$ are defined as

$$\alpha_{\ell,m} = \mathbb{E}\left[(z - \mathbb{E}[z])^{\ell}(z - \mathbb{E}[z])^{*m}\right], \ell, m \in \mathbb{R} \geq 0$$

With $\sigma^2 = \alpha_{1,1}$, *Standardized moments* $\varrho_{\ell,m}$ can then be found as

$$\varrho_{\ell,m} = \frac{\alpha_{\ell,m}}{\sigma^{\ell+m}}$$

Leading to the CSK (Complex Signal Kurtosis) RFI test statistic used [4].

$$C_K = \frac{\varrho_{2;2} - 2 - \left|\varrho_{2;0}\right|^2}{1 + \frac{1}{2}\left|\varrho_{2;0}\right|^2}$$

Algorithm Simulation and Verification

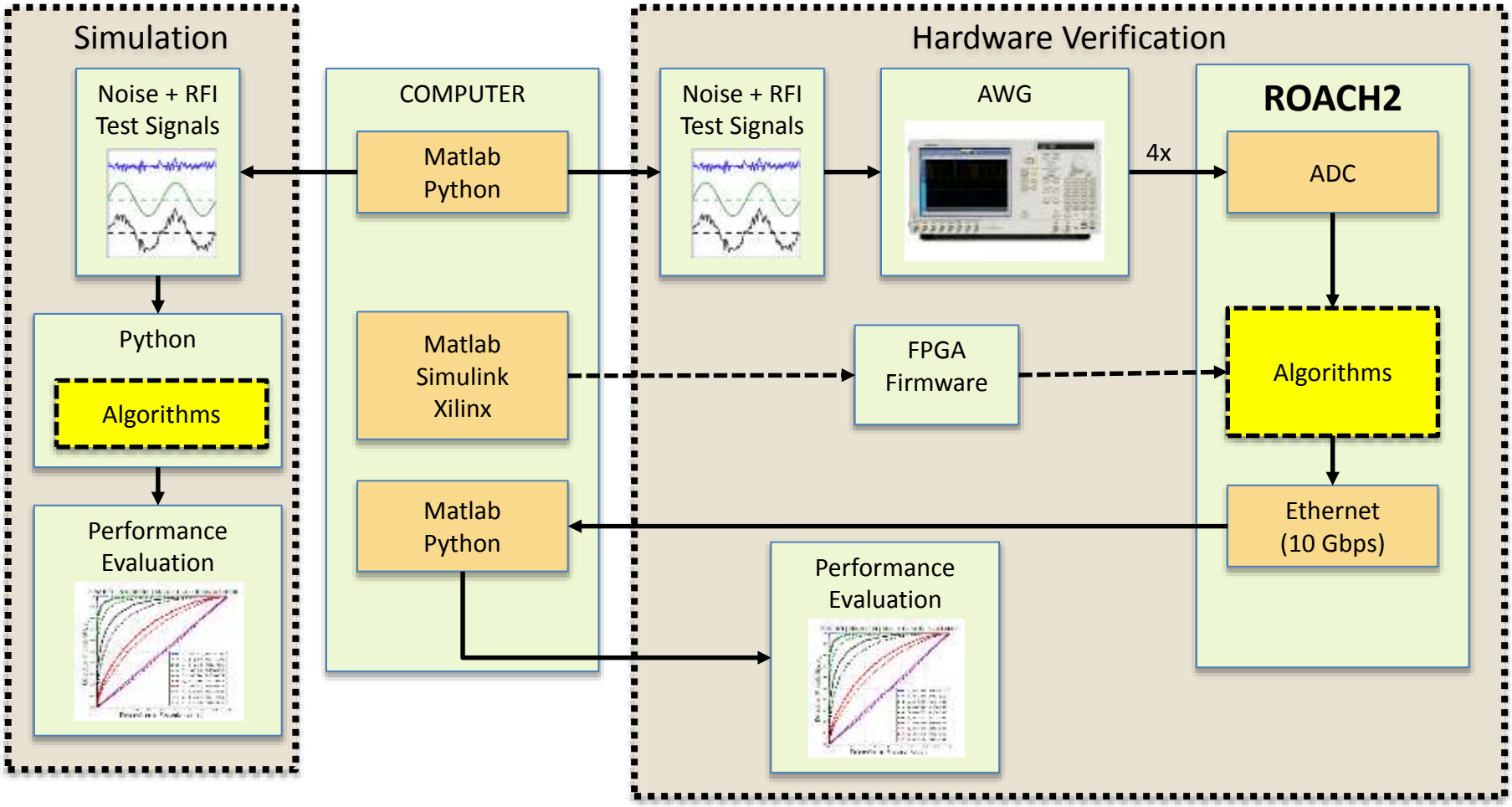

ROACH2 Implementation of RFI Detection Algorithms

- As a base line, a modified version of the Soil Moisture Active Passive Mission (SMAP) digital signal processing architecture was implemented in the Reconfigurable Open Architecture Computing Hardware (ROACH2) with a bandwidth of 24 MHz and verified using test signals generated. [5,6]
- This architecture provided outputs for the real and complex kurtosis statistical computations at 24 MHz
- The architecture was then implemented and verified at 200 MHz bandwidth in the ROACH2
- The real and complex kurtosis were also computed using outputs from the 200 MHz bandwidth architecture

ROACH2 Hardware Description

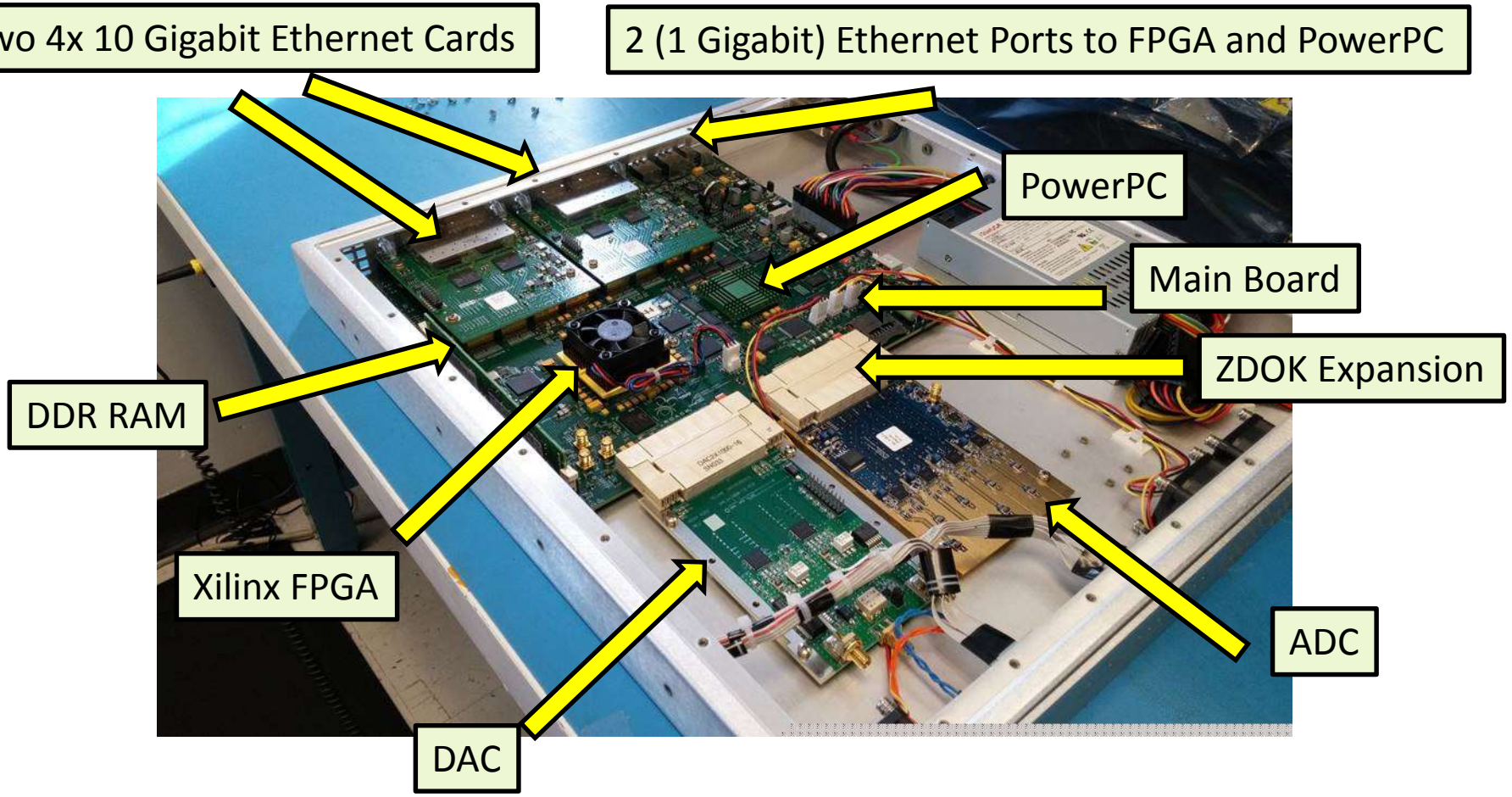

SMAP Modified DSP Architecture at Faster Sampling Rate

- The FPGA clock speed was increased from 96 MHz to 200 MHz (ratio of 1 : 2.08)
- The ADC sampling rate was increased from 96 MHz to 800 MHz (ratio of 1 : 8.33)
  - Two ADCs clocked at 800 MSPS each
  - Each channel has a 1 : 4 SERDES (Serializer/Deserializer) reception
    - The FPGA reads four samples from each channel every clock cycle
- The DSP (Digital Signal Processing) algorithm had to be parallelized to handle the data throughput
  - A SERDES block natively implements the first stage of a polyphase decomposition
  - The down-sampling is now performed before modulation and filtering, but the entire system input / output is identical

Modified DSP Architecture at Faster Sampling Rate

Effective Analog of DDC From SMAP DSP Architecutre

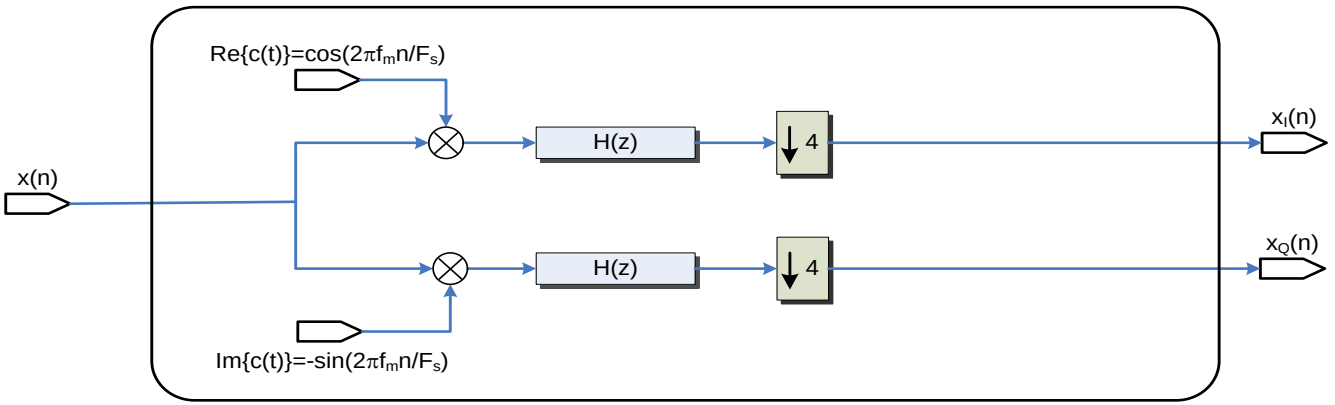

Equivalent Polyphase Decomposition for Serdes Inputs

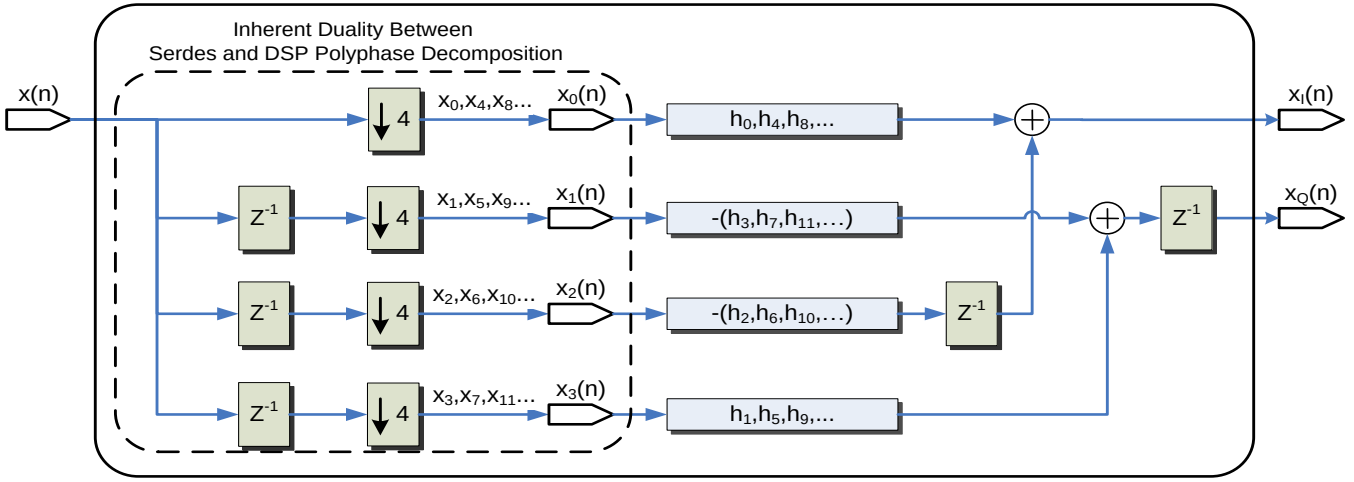

Wideband RFI Telemetry - RSK

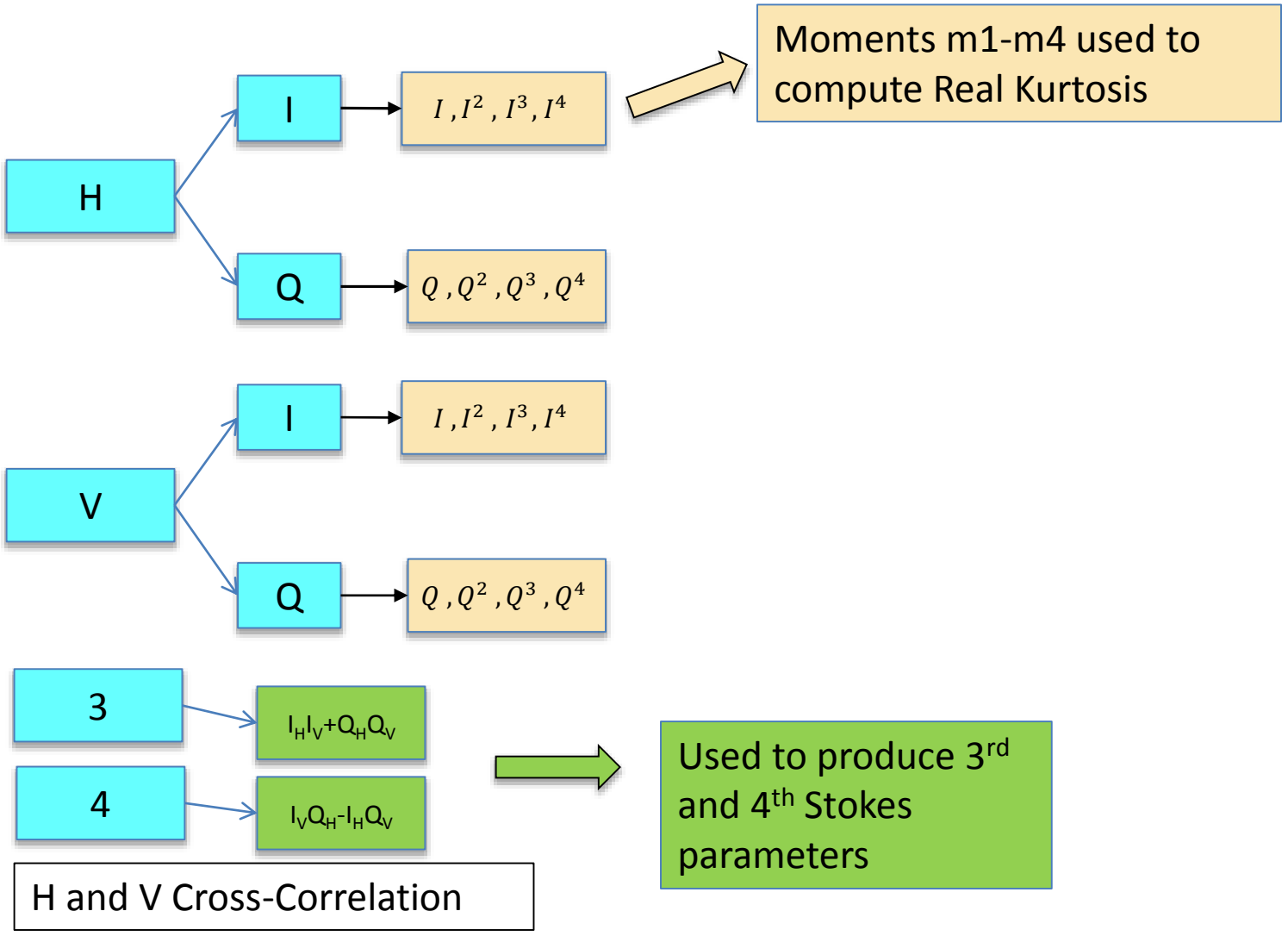

Wideband RFI Telemetry - CSK

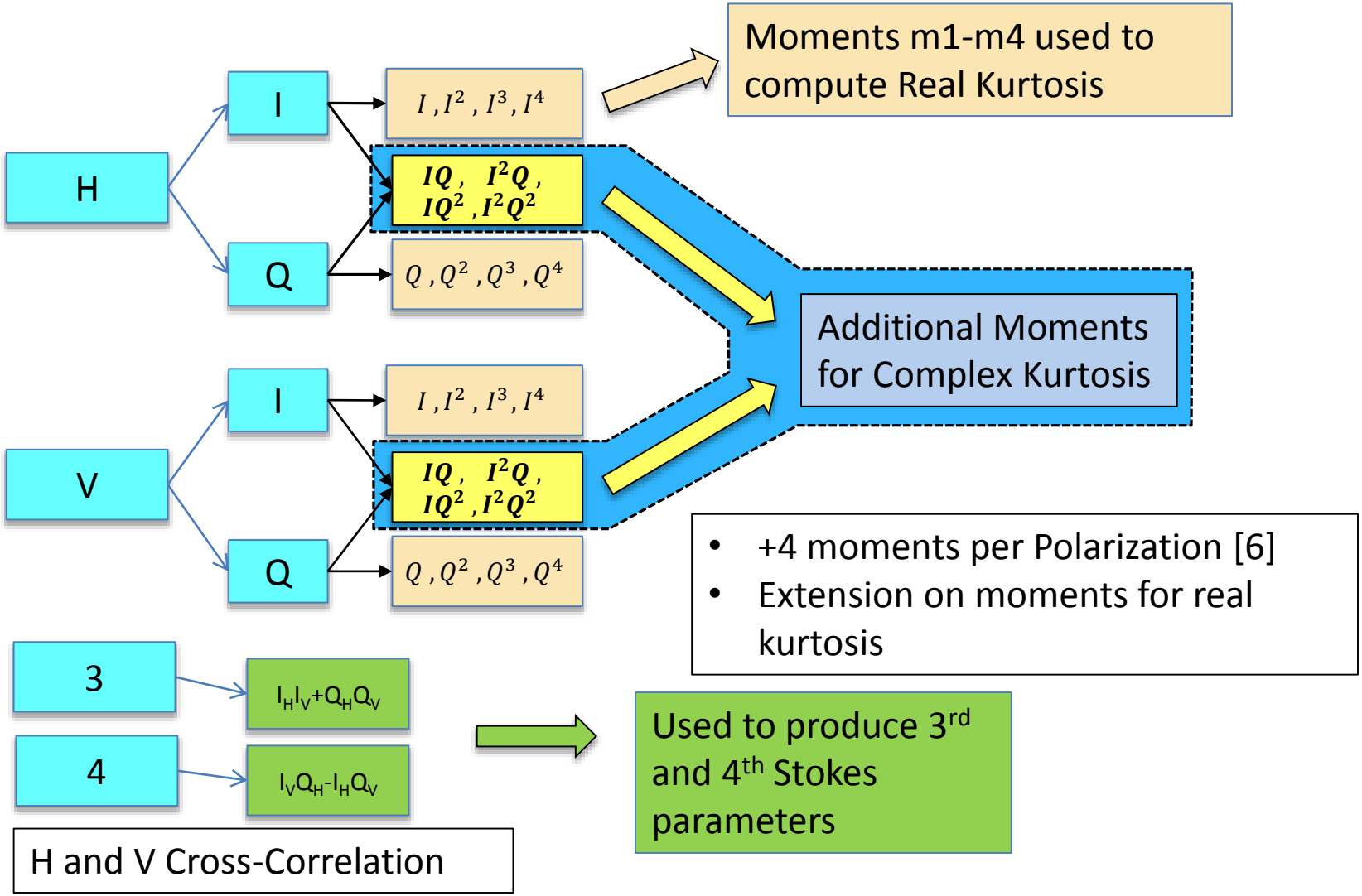

ROC Curves and AUC

- Each point on an ROC curve can be represented by the set {FAR, PD}
  - {False alarm Rate , Probability of Detection}
- ROC curves will generate from (0,0) to (1,1) by varying the threshold
- Poor detectors are close to the 1:1 line
- Better detectors show higher PD and smaller FAR
- **Figure of Merit = Area Under Curve (AUC)**
  - 0.5≤AUC ≤1
  - When AUC = 0.5 detector does not work
  - When AUC = 1 the detector works perfectly

Better Detection

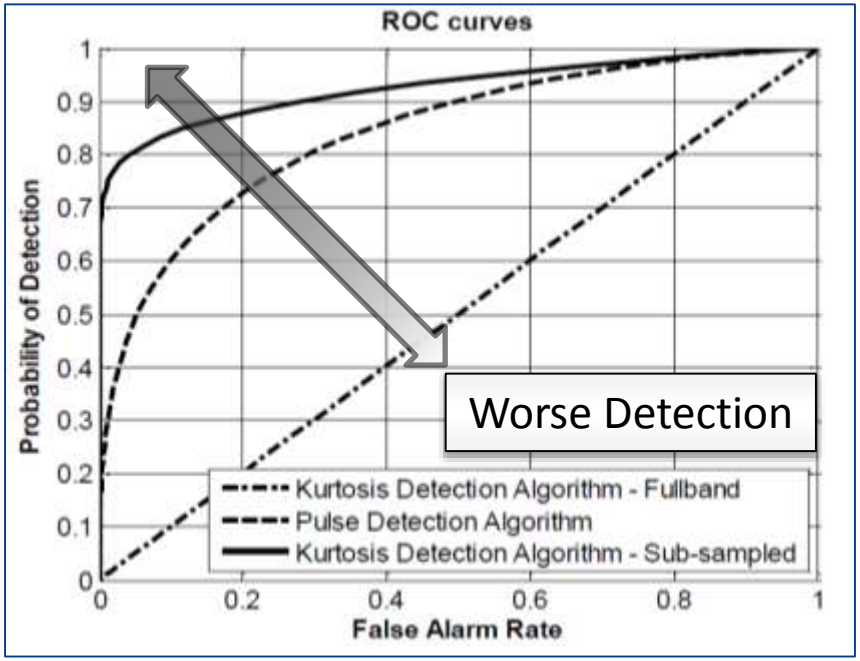

ROC curve example, from [7].

AUC = 1 ⟷ AUC = 0.5

Better Detection

Worse Detection

Simulation Results

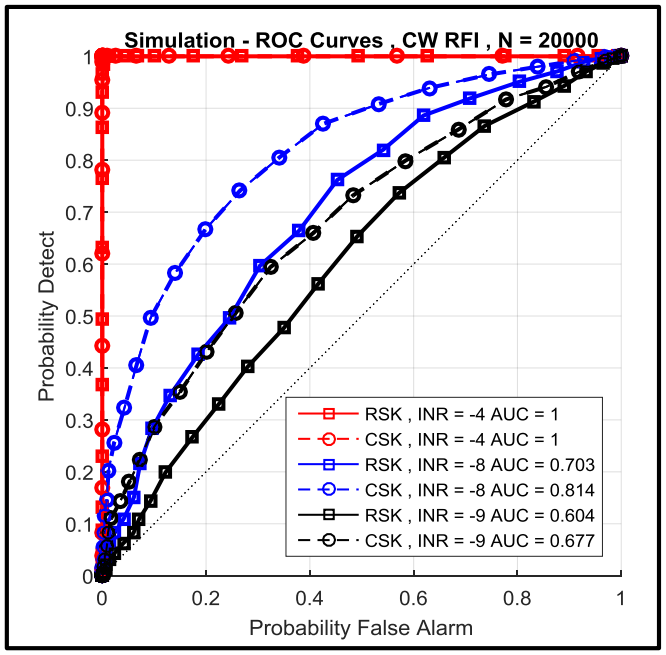

CW Modulation
CSK is outperforming RSK

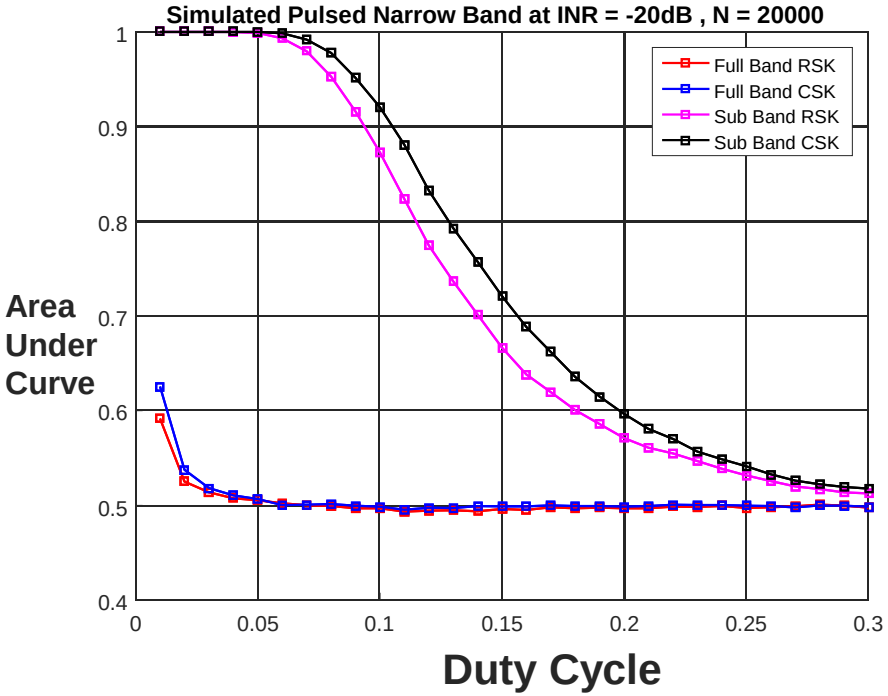

Smaller duty cycles are easier to detect; sub-banding improves detection [6].

Simulation Results

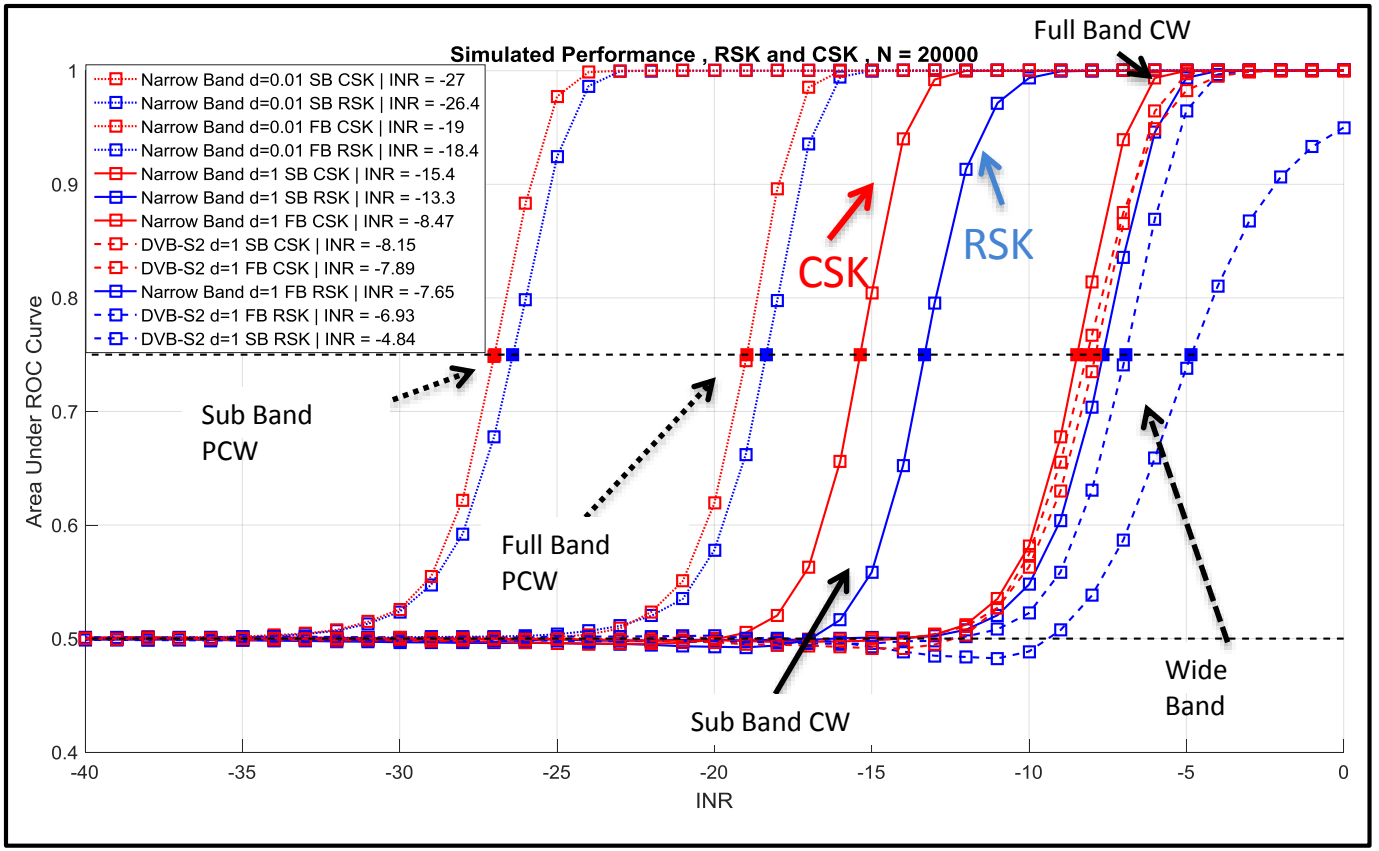

- Wide Band revers to QPSK with a RRCOS filter simulating a DVB-S2 Channel,
  - Band occupancy = 0.0375 Fs , Carrier = 0.175 Fs
- Using Monte Carlo Simulations, INR is swept is for different types of RFI modulations.
- Algorithms are compared by looking at INR when AUC = 0.75 .
- CSK shows improved detection over RSK.
- PCW is easiest to detect. Wideband is hardest to detect [6].

AUC Results: Kurtosis As Detector

Kurtosis yields poor detector for CW and Wide Band RFI

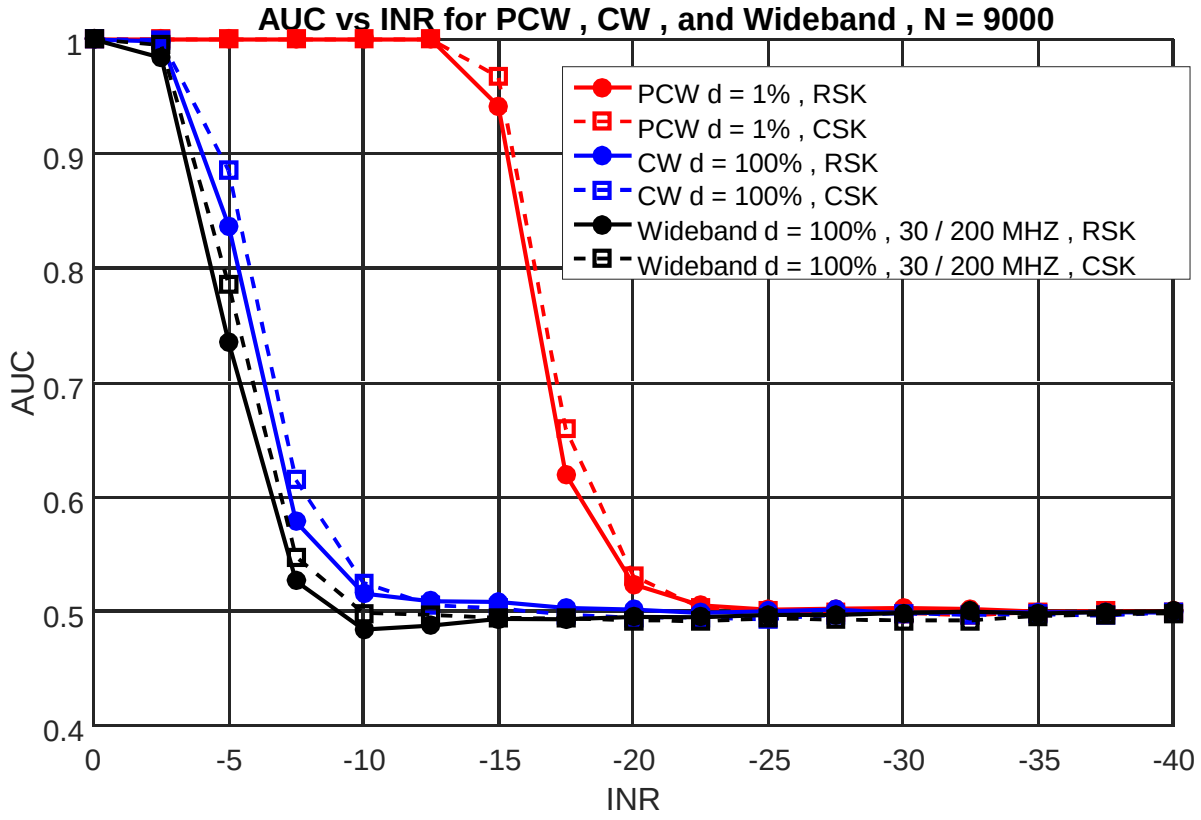

Kurtosis yields good detection for PCW (Such as RADAR)

Sub-banding Verification with Chirp

- 200 MHz BW

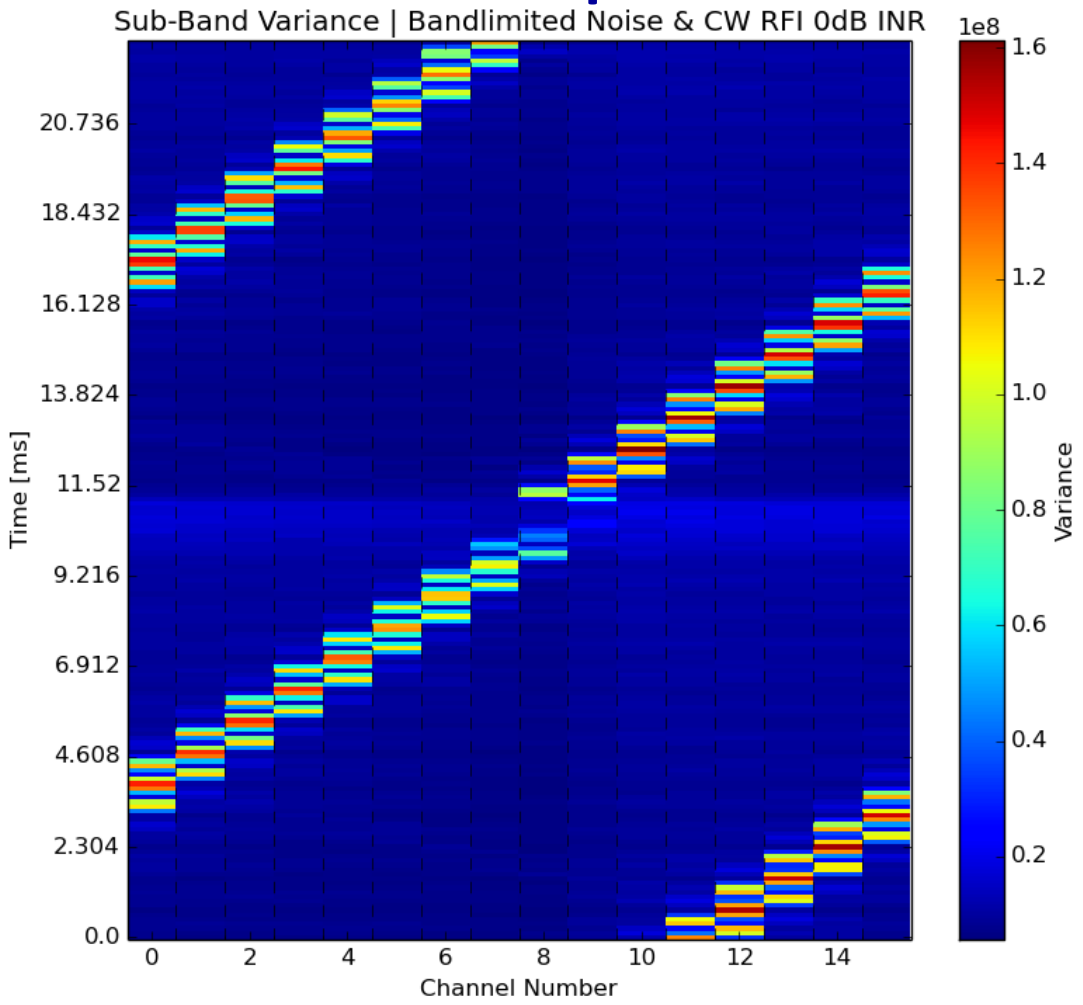

Channelized Complex Kurtosis

Visual Verification of channelization.

Deviation away from 0 means interference is detected.

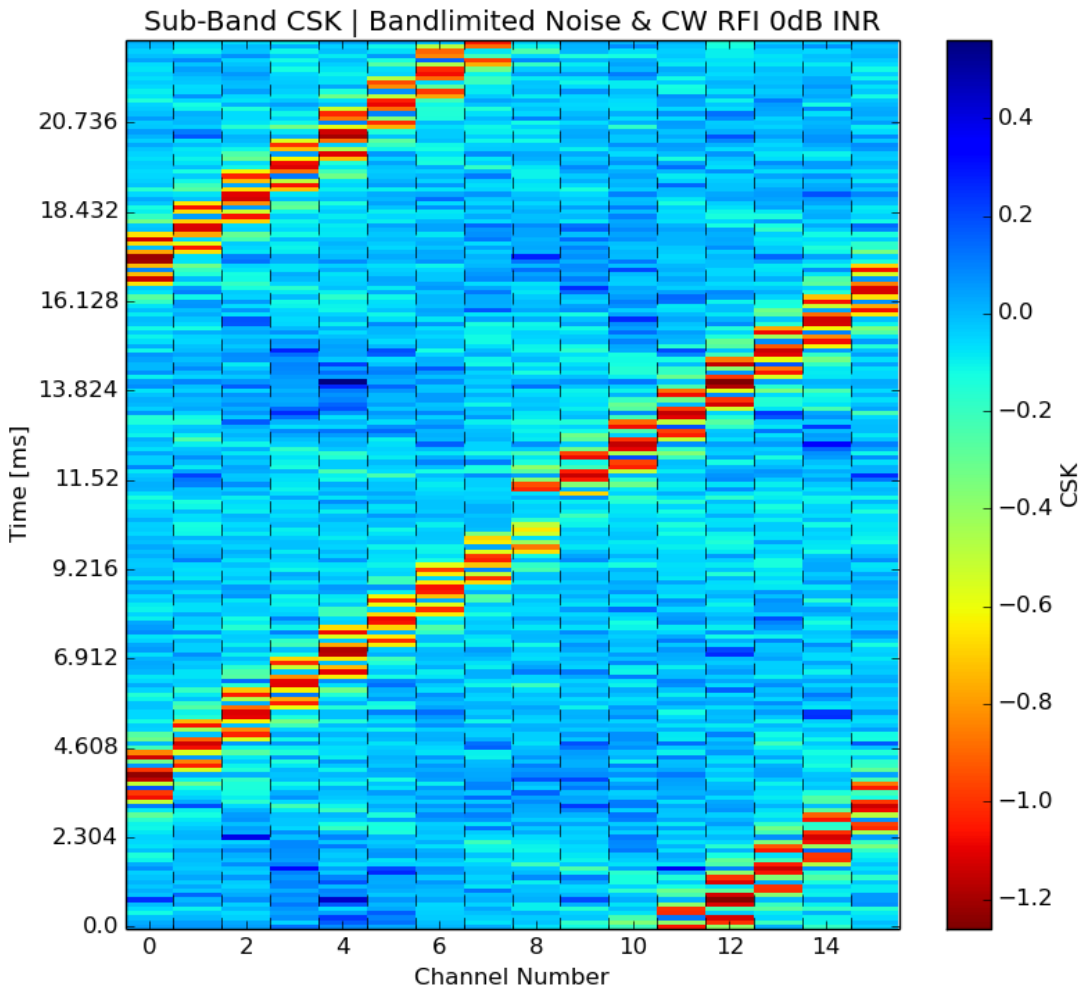

Hardware Results

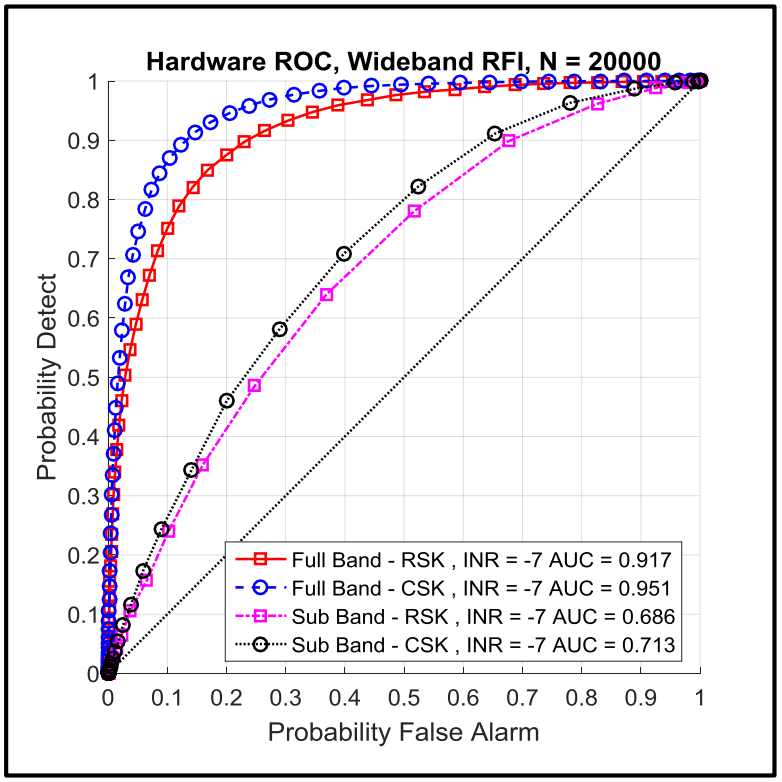

Sub banding decreased detection on wide band RFI

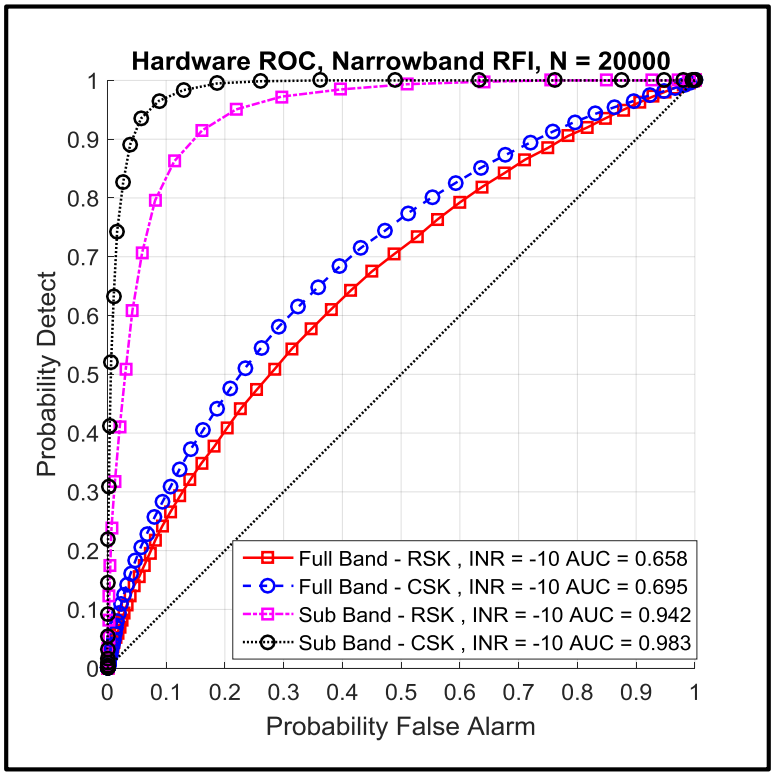

Sub banding improved detection on narrow band RFI

Independent Component Analysis

- ICA [8] uses higher order statistics to perform blind source separation
- This suggests it may be useful for separating RFI from Gaussian noise in the radiometry context.
- We assume noise and RFI are statistically independent sources, mixing is linear, sources are non Gaussian
- Mixture model: **x = As**, observe **x**
- $\hat{s}$ = **Wx**, $\hat{s}$ is the estimated independent source

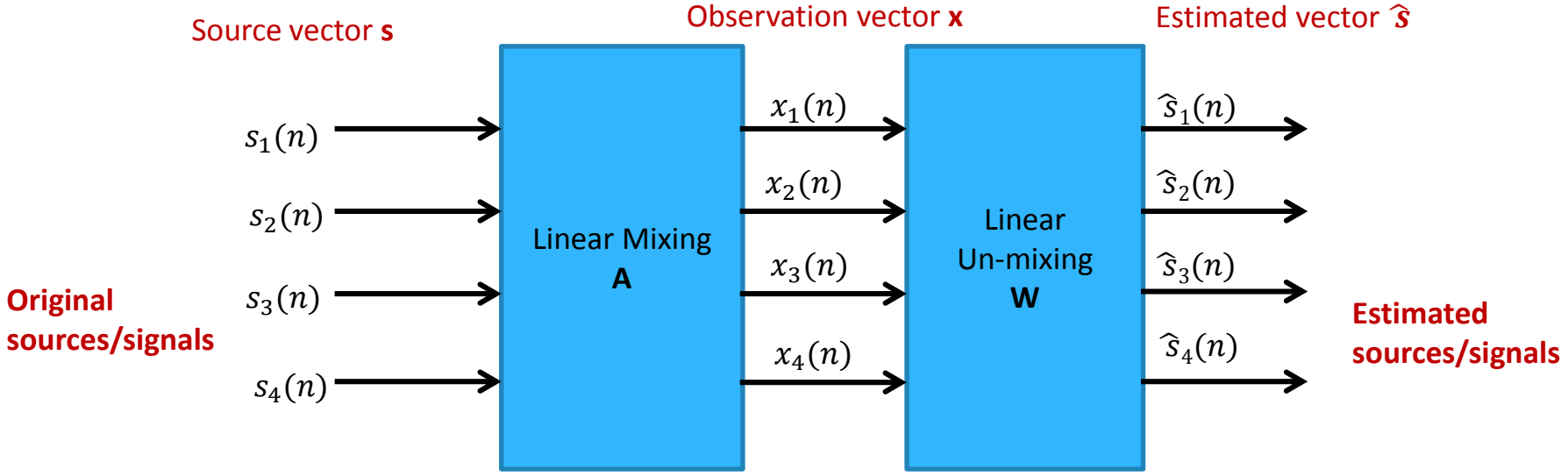

ICA Algorithm

$$\begin{bmatrix} x_{\mathrm{HI}}[0] & x_{\mathrm{HI}}[1] & \dots & x_{\mathrm{HI}}[N-1] \\ x_{\mathrm{HQ}}[0] & x_{\mathrm{HQ}}[1] & \dots & x_{\mathrm{HQ}}[N-1] \\ x_{\mathrm{VI}}[0] & x_{\mathrm{VI}}[1] & \dots & x_{\mathrm{VI}}[N-1] \\ x_{\mathrm{VQ}}[0] & x_{\mathrm{VQ}}[1] & \dots & x_{\mathrm{VQ}}[N-1] \end{bmatrix} = \begin{bmatrix} a_{00} & a_{01} & a_{02} & a_{03} \\ a_{10} & a_{11} & a_{12} & a_{13} \\ a_{20} & a_{21} & a_{22} & a_{23} \\ a_{30} & a_{31} & a_{32} & a_{33} \end{bmatrix} \begin{bmatrix} s_{0,0} & s_{0,1} & s_{0,2} & s_{0,3} & \dots & s_{0,N-1} \\ s_{1,0} & s_{1,1} & s_{1,2} & s_{1,3} & \dots & s_{1,N-1} \\ s_{2,0} & s_{2,1} & s_{2,2} & s_{2,3} & \dots & s_{2,N-1} \\ s_{3,0} & s_{3,1} & s_{2,2} & s_{3,3} & \dots & s_{3,N-1} \end{bmatrix}$$

Observations | Mixing Matrix | Independent Components

Find A matrix to transform X into S

- Actual Signals, **S ,** are mixed by mixing matrix, A, and observed as X
- We pick a matrix , $\widehat{\mathbf{W}}$, that gives us back our estimated signals, $\widehat{\mathbf{S}}$

$$\boldsymbol{x} = \boldsymbol{As}$$
$$\boldsymbol{W} = \boldsymbol{A}^{-1}$$
$$\mathbf{s} = \mathbf{Wx}$$

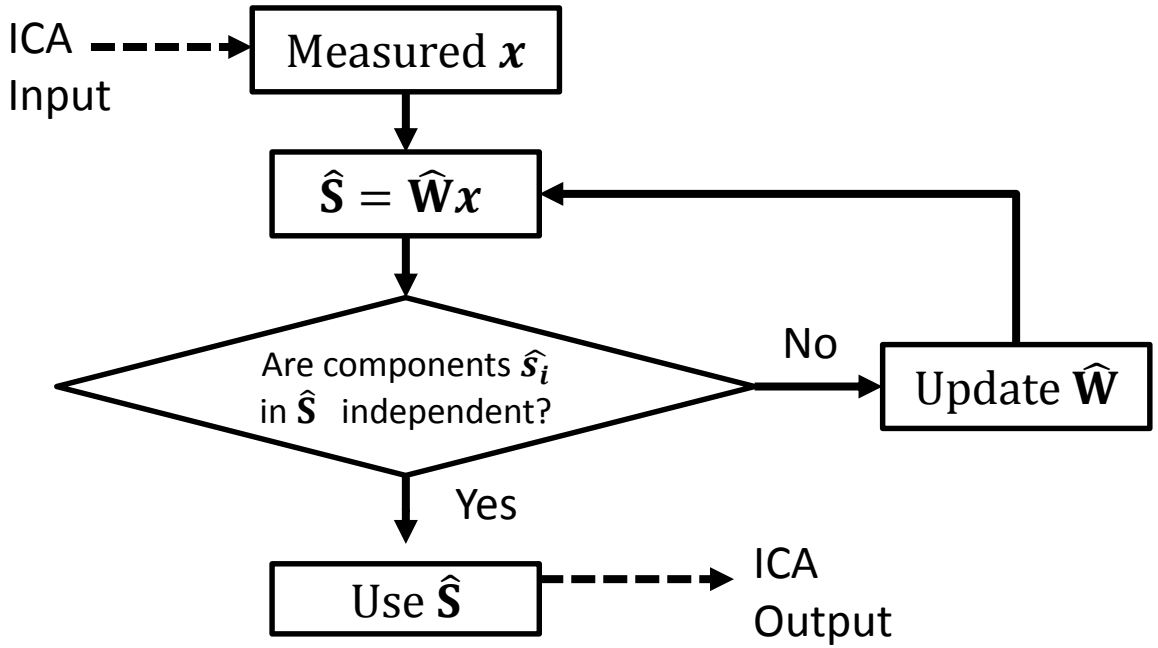

Signal Model

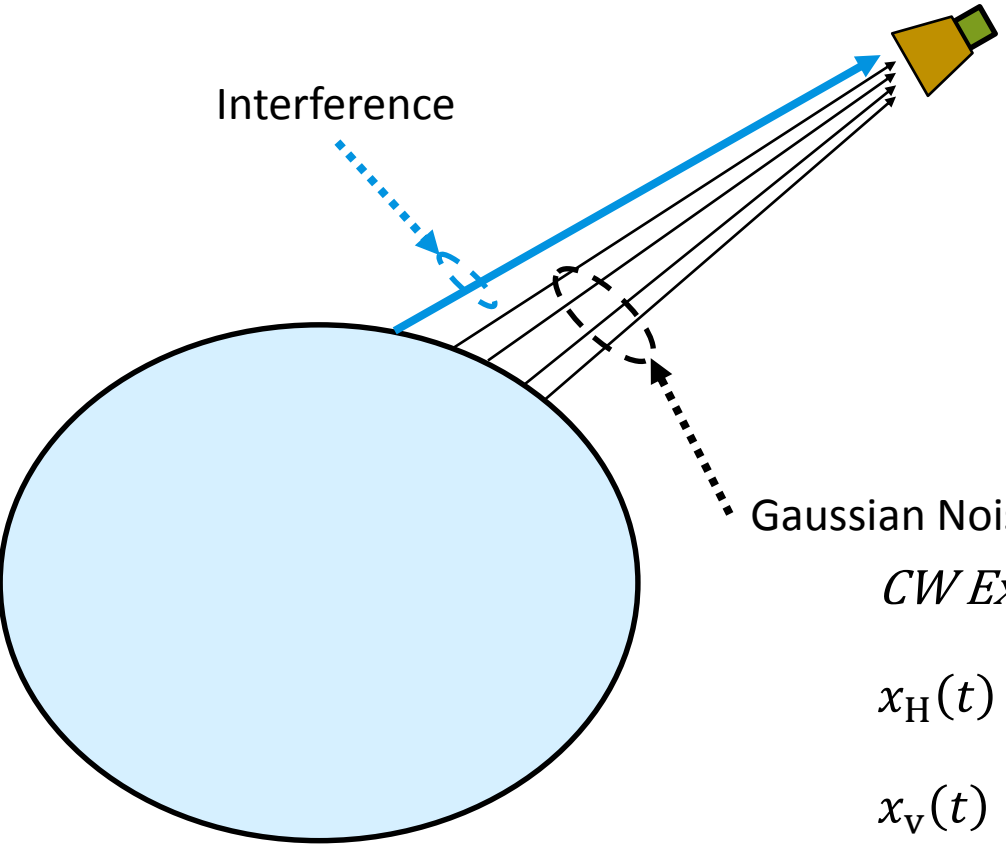

- Assumptions
  - Gaussian Noise between H and V polarizations is Independent and Uncorrelated
  - Interference is circularly polarized

$$x_{\mathrm{H}}(t) = \mathrm{rfi}(t) + \mathrm{wgn}_1(t)$$

$$x_{\mathrm{V}}(t) = \mathrm{rfi}(t)\, e^{-\left(\frac{i\pi}{2}\right)} + \mathrm{wgn}_2(t)$$

CW Example:

$$x_{\mathrm{H}}(t) = (a\sin(\omega_0 t) + \mathrm{w}_2(t)) * h(t)$$

$$x_{\mathrm{v}}(t) = (a\sin(\omega_0 t - \pi/2) + \mathrm{w}_2(t)) * h(t)$$

ICA RFI Detection

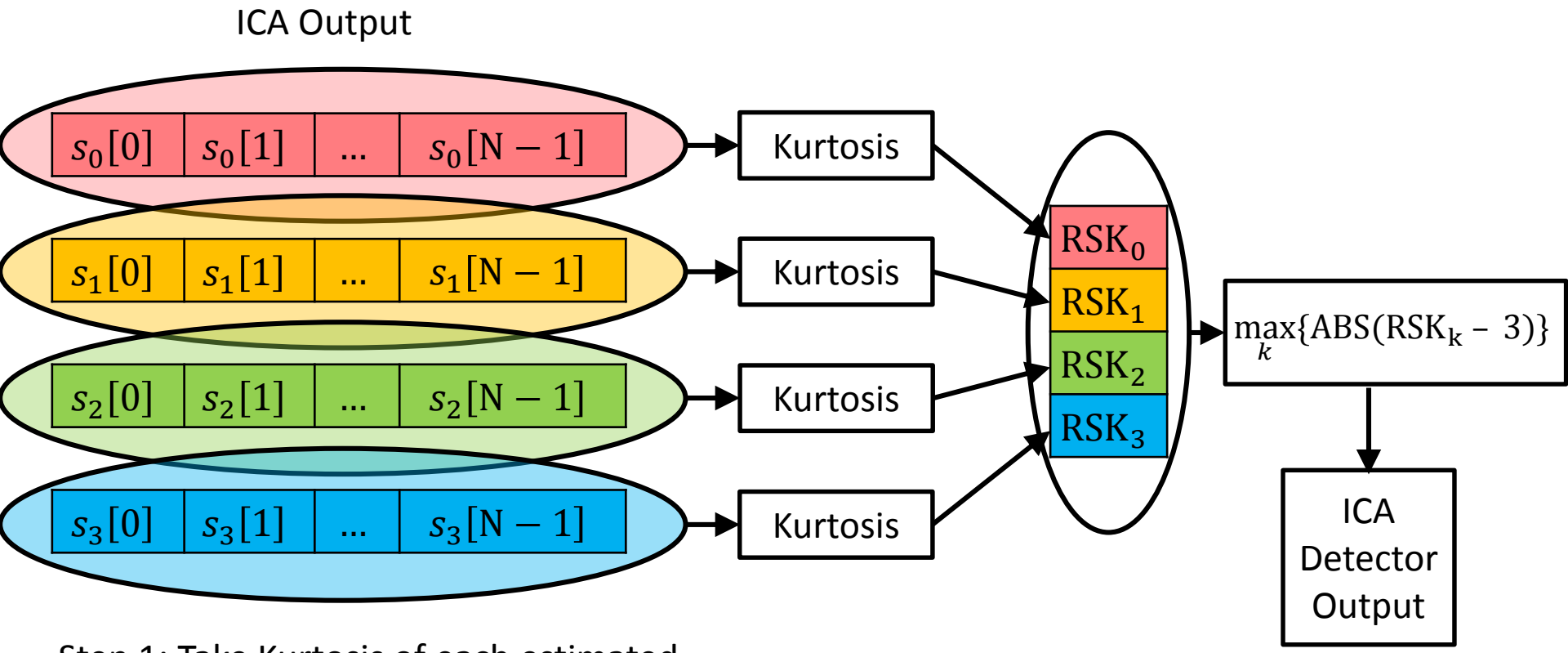

Step 1: Take Kurtosis of each estimated independent component vector

Step 2: Select the kurtosis value that deviated the furthest from 3

AUC Results- ICA Performance - PCW

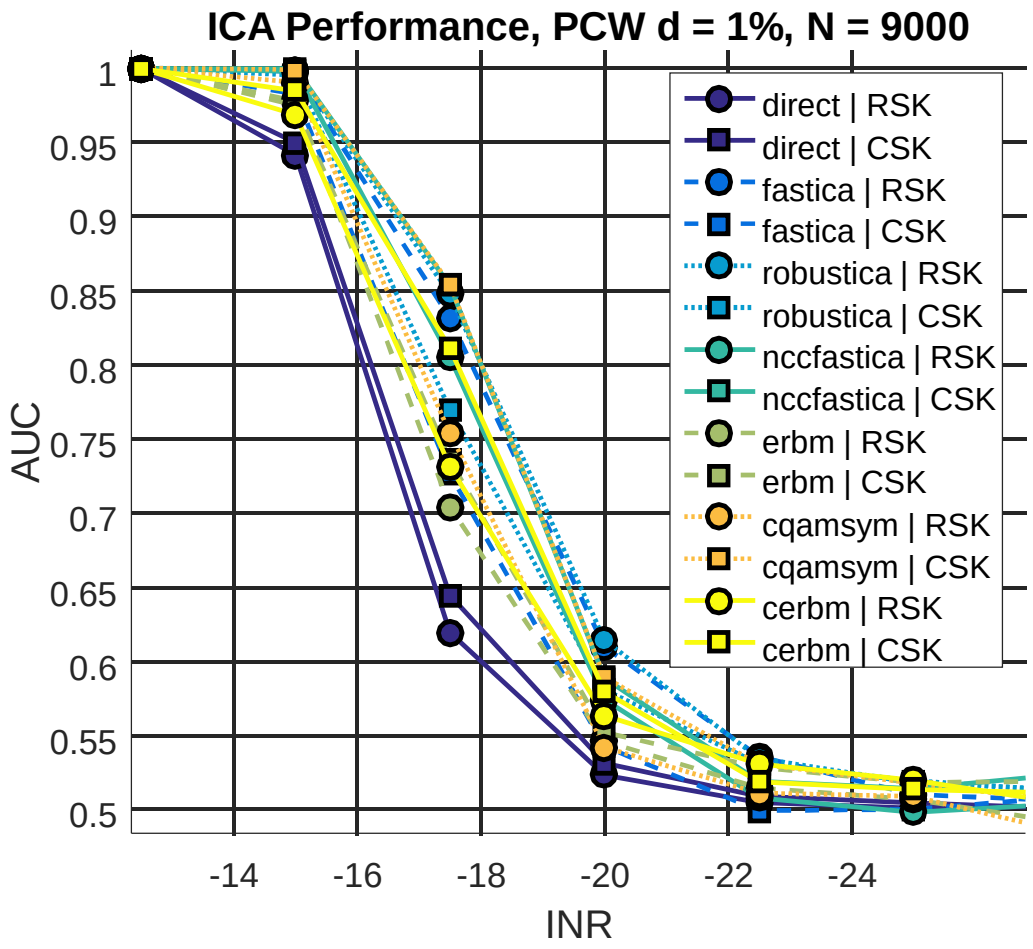

+2dB INR Gain,
Real Signal Kurtosis with FastICA performs just as well as other algorithms for PCW

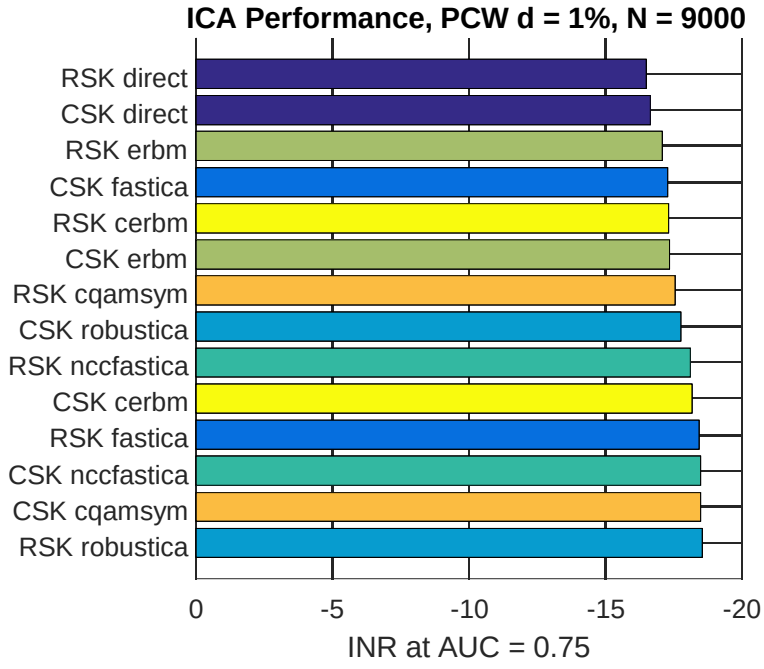

Various ICA algorithms are tested [9,10,11,12,13,14,15,16,17].
No ICA pre-processing is done on 'direct' data sets.

RSK = Real Signal Kurtosis
CSK = Complex Signal Kurtosis

AUC Results- ICA Performance - CW

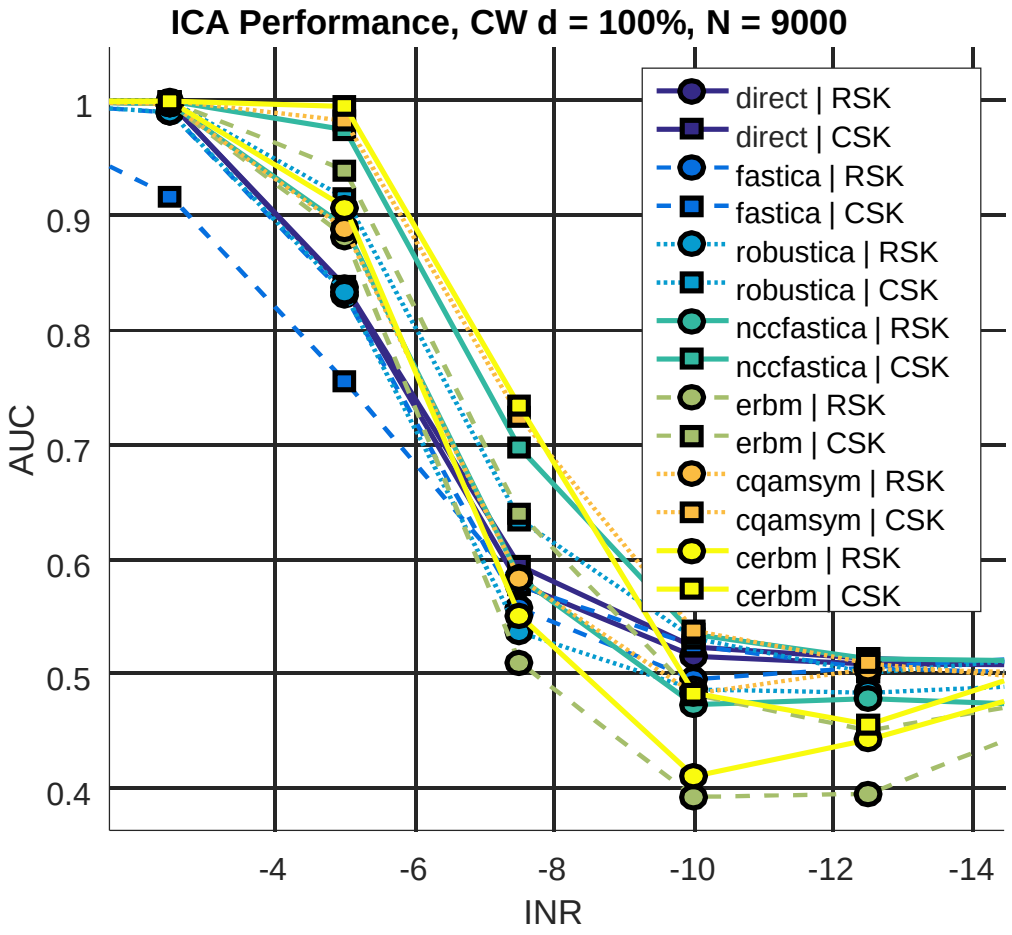

+2dB INR Gain,
Complex Signal Kurtosis with
Complex ICA Algorithms
Performs Best on CW

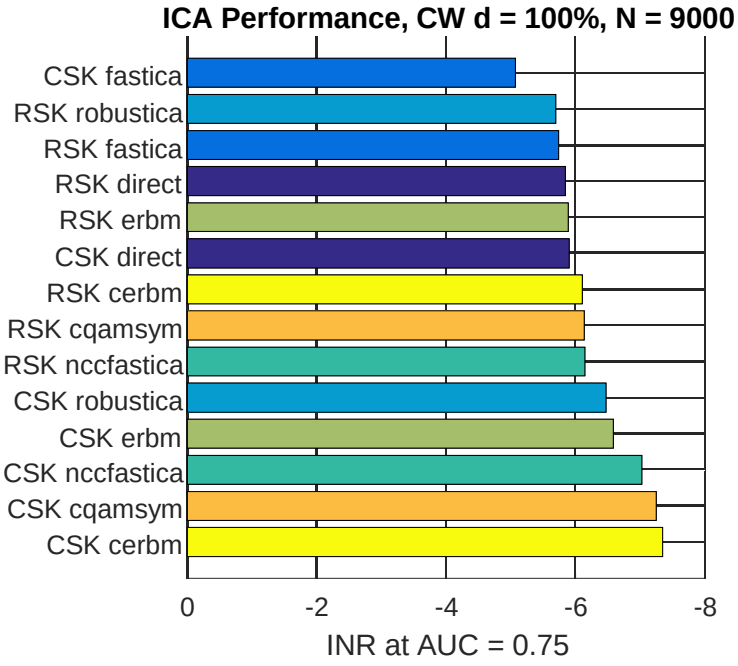

Various ICA algorithms are tested [9,10,11,12,13,14,15,16,17].
No ICA pre-processing is done on 'direct' data sets.

RSK = Real Signal Kurtosis
CSK = Complex Signal Kurtosis

AUC Results – ICA Performance – Wide Band

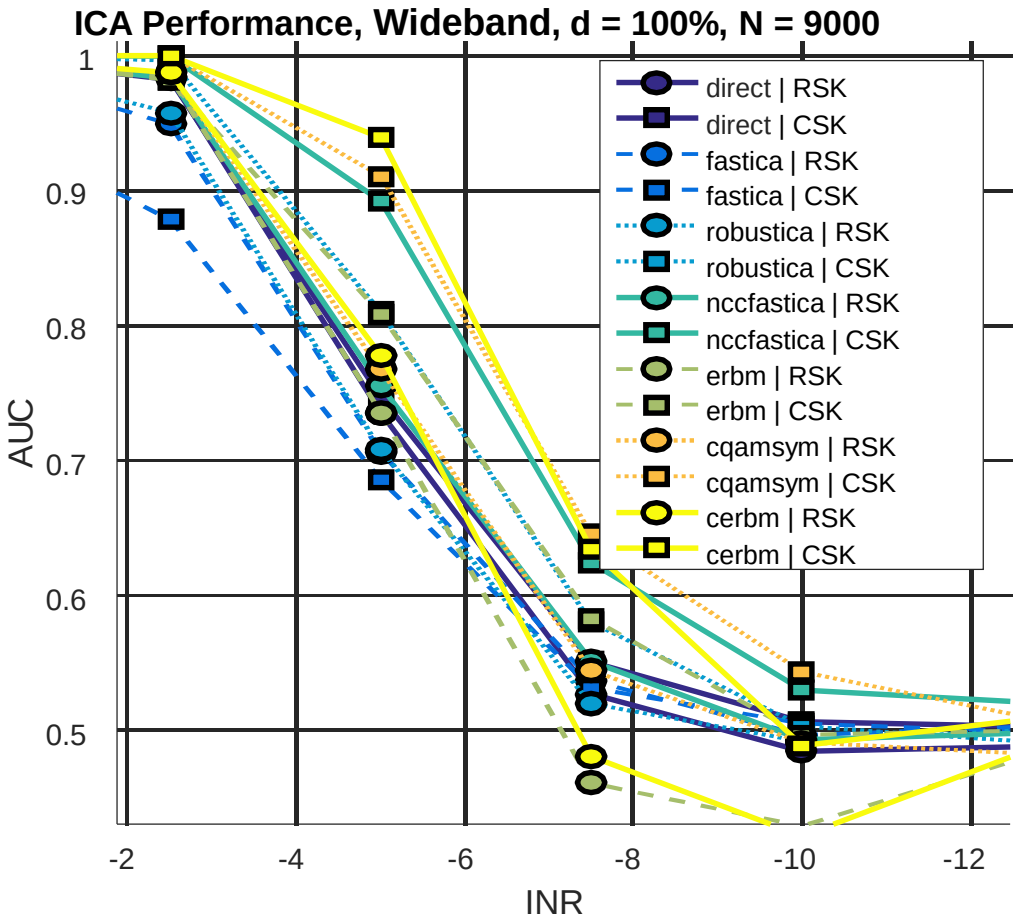

+2dB INR Gain,
Complex Signal Kurtosis with
Complex ICA Algorithms
Performs Best on Wideband

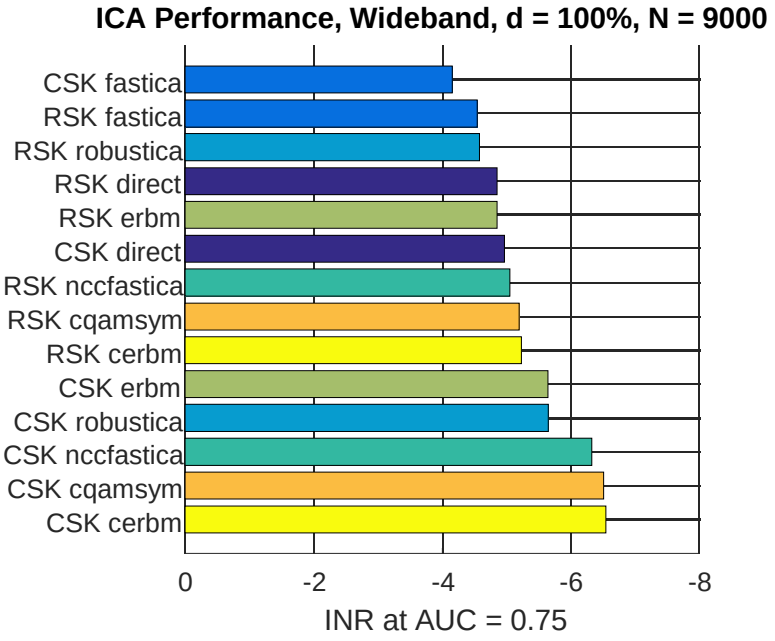

Various ICA algorithms are tested [9,10,11,12,13,14,15,16,17].
No ICA pre-processing is done on 'direct' data sets.

RSK = Real Signal Kurtosis
CSK = Complex Signal Kurtosis

Conclusions

- CSK provides better detection over RSK
- ICA allowed equivalent detection at about 2dB lower INR when used as a preprocessor for RSK and CSK normality tests
- ICA performance mainly limited due to an underdetermined observation matrix
- May be more suitable to systems with a greater number of observation channels

ICA Algorithms Used

- Fast ICA (FASTICA) [9,15]
  - A. Hyvärinen. “Fast and Robust Fixed-Point Algorithms for Independent Component Analysis”, IEEE Transactions on Neural Networks 10(3):626-634, 1999.
- Robust ICA (ROBUSTICA) [10,16]
  - V. Zarzoso and P. Comon, "Robust Independent Component Analysis by Iterative Maximization of the Kurtosis Contrast with Algebraic Optimal Step Size", IEEE Transactions on Neural Networks, Vol. 21, No. 2, February 2010, pp. 248-261.
- Non Circular Complex Fast ICA (NCCFASTICA) [11,17]
  - Mike Novey and T. Adali, "On Extending the complex FastICA algorithm to noncircular sources" IEEE Trans. Signal Processing, vol. 56, no. 5, pp. 2148-2154, May 2008.
- Entropy Rate Bound Minimization (ERBM) [12,17]
  - X.-L. Li, and T. Adali, "Blind spatiotemporal separation of second and/or higher-order correlated sources by entropy rate minimization," in Proc. IEEE Int. Conf. Acoust., Speech, Signal Processing (ICASSP), Dallas, TX, March 2010.
- Complex Quadrature Amplitude Modulation (CQAMSYM) [13,17]
  - Mike Novey and T. Adali, "Complex Fixed-Point ICA Algorithm for Separation of QAM Sources using Gaussian Mixture Model" in IEEE Conf. ICASSP 2007
- Complex Entropy Rate Bound Minimization (CERBM) [14,17]
  - G.-S. Fu, R. Phlypo, M. Anderson, and T. Adali, "Complex Independent Component Analysis Using Three Types of Diversity: Non-Gaussianity, Nonwhiteness, and Noncircularity," IEEE Trans. Signal Processing, vol. 63, no. 3, pp. 794-805, Feb. 2015.

References

1) Draper, David W., “Report on GMI Special Study #15: Radio Frequency Interference” , Ball Aerospace and Technologies Corp., Jan 16, 2015

2) De Roo, R.D.; Misra, S.; Ruf, C.S., "Sensitivity of the Kurtosis Statistic as a Detector of Pulsed Sinusoidal RFI," in Geoscience and Remote Sensing, IEEE Transactions on , vol.45, no.7, pp.1938-1946, July 2007

3) J. Piepmeier, J. Johnson, P. Mohammed, D. Bradley, C. Ruf, M. Aksoy, R. Garcia, D. Hudson, L. Miles,and M. Wong, “Radio-frequency interference mitigation for the soil moisture active passive microwave radiometer,” IEEE Transactions on Geoscience and Remote Sensing, vol. 52, no. 1, pp. 761–775, January 2014.

4) Bradley, D.; Morris, J.M.; Adali, T.; Johnson, J.T.; Aksoy, M., "On the detection of RFI using the complex signal kurtosis in microwave radiometry," in Microwave Radiometry and Remote Sensing of the Environment (MicroRad), 2014 13th Specialist Meeting on , vol., no., pp.33-38, 24-27 March 2014

5) D. C. Bradley, A. J. Schoenwald, M. Wong, P. N. Mohammed and J. R. Piepmeier, "Wideband digital signal processing test-BED for radiometric RFI mitigation," 2015 IEEE International Geoscience and Remote Sensing Symposium (IGARSS), Milan, 2015, pp. 3489-3492.

6) A. J. Schoenwald, D. C. Bradley, P. N. Mohammed, J. R. Piepmeier and M. Wong, "Performance analysis of a hardware implemented complex signal kurtosis radio-frequency interference detector," 2016 14th Specialist Meeting on Microwave Radiometry and Remote Sensing of the Environment (MicroRad), Espoo, 2016, pp. 71-75.

7) S. Misra, P. N. Mohammed, B. Guner, C. S. Ruf, J. R. Piepmeier and J. T. Johnson, "Microwave Radiometer Radio-Frequency Interference Detection Algorithms: A Comparative Study," in IEEE Transactions on Geoscience and Remote Sensing, vol. 47, no. 11, pp. 3742-3754, Nov. 2009.

8) A. Hyvärinen and E. Oja. Independent component analysis: algorithms and applications. Neural Networks 13, 4-5 (May 2000), 411-430

9) A. Hyvärinen. “Fast and Robust Fixed-Point Algorithms for Independent Component Analysis”, IEEE Transactions on Neural Networks 10(3):626-634, 1999.

10) V. Zarzoso and P. Comon, "Robust Independent Component Analysis by Iterative Maximization of the Kurtosis Contrast with Algebraic Optimal Step Size", IEEE Transactions on Neural Networks, Vol. 21, No. 2, February 2010, pp. 248-261.

11) Mike Novey and T. Adali, "On Extending the complex FastICA algorithm to noncircular sources" IEEE Trans. Signal Processing, vol. 56, no. 5, pp. 2148-2154, May 2008.

12) X.-L. Li, and T. Adali, "Blind spatiotemporal separation of second and/or higher-order correlated sources by entropy rate minimization," in Proc. IEEE Int. Conf. Acoust., Speech, Signal Processing (ICASSP), Dallas, TX, March 2010.

13) Mike Novey and T. Adali, "Complex Fixed-Point ICA Algorithm for Separation of QAM Sources using Gaussian Mixture Model" in IEEE Conf. ICASSP 2007

14) G.-S. Fu, R. Phlypo, M. Anderson, and T. Adali, "Complex Independent Component Analysis Using Three Types of Diversity: Non-Gaussianity, Nonwhiteness, and Noncircularity," IEEE Trans. Signal Processing, vol. 63, no. 3, pp. 794-805, Feb. 2015.

15) ICA and BSS Group, Aalto University, Matlab Resources, http://research.ics.aalto.fi/ica/fastica/

16) Vicente Zarzoso, Institut Universitaire de France , Robust ICA, Matlab Resources, http://www.i3s.unice.fr/~zarzoso/robustica.html

17) Machine Learning for Signal Processing Laboratory, University of Maryland Baltimore County , Matlab Resources, http://mlsp.umbc.edu/resources.html